

Please cite the Published Version

Palanisamy, S, Thangavelu, K, Chen, SM, Gnanaprakasam, P, Velusamy, V and Liu, XH (2016) Preparation of chitosan grafted graphite composite for sensitive detection of dopamine in biological samples. *Carbohydrate Polymers*, 151. pp. 401-407. ISSN 0144-8617

DOI: <https://doi.org/10.1016/j.carbpol.2016.05.076>

Publisher: Elsevier

Version: Accepted Version

Downloaded from: <https://e-space.mmu.ac.uk/619514/>

Usage rights:  [Creative Commons: Attribution-Noncommercial-No Derivative Works 4.0](https://creativecommons.org/licenses/by-nc-nd/4.0/)

Additional Information: This is an Author Accepted Manuscript of a paper accepted for publication in *Carbohydrate Polymers*, published by and copyright Elsevier.

Enquiries:

If you have questions about this document, contact openresearch@mmu.ac.uk. Please include the URL of the record in e-space. If you believe that your, or a third party's rights have been compromised through this document please see our Take Down policy (available from <https://www.mmu.ac.uk/library/using-the-library/policies-and-guidelines>)

1 **Preparation of chitosan grafted graphite composite for sensitive detection of dopamine in**
2 **biological samples**

3 Selvakumar Palanisamy¹, Kokulnathan Thangavelu¹, Shen-Ming Chen^{*1}, P. Gnanaprakasam²,
4 Vijayalakshmi Velusamy³, Xiao-Heng Liu^{4**}

5 ¹Electroanalysis and Bioelectrochemistry Lab, Department of Chemical Engineering and
6 Biotechnology, National Taipei University of Technology, No.1, Section 3, Chung-Hsiao East
7 Road, Taipei 106, Taiwan (R.O.C).

8 ²Department of Nanoscience and Nanotechnology, Karunya University, Coimbatore 64114, India
9 Corresponding author. Tel: +886 2270 17147; fax: +886 2270 25238.

10 ³Division of Electrical and Electronic Engineering, School of Engineering, Manchester
11 Metropolitan University, Manchester – M1 5GD, United Kingdom.

12 ⁴Key Laboratory of Education Ministry for Soft Chemistry and Functional Materials, Nanjing
13 University of Science and Technology, Nanjing 210094, China

14

15 Corresponding author. Tel: +886 2270 17147; fax: +886 2270 25238.

16 *E-mail address: smchen78@ms15.hinet.net (S.M. Chen); xhliu@mail.njust.edu.cn (X.H. Liu)

17

18

19 **Abstract**

20 The accurate detection of dopamine (DA) levels in biological samples such as human
21 serum and urine samples are essential indicators in medical diagnostics. In this work, we describe
22 the preparation of chitosan (CS) biopolymer grafted graphite (GR) composite for the sensitive and
23 lower potential detection of DA in its sub micromolar levels. The composite modified electrode
24 has been used for the detection of DA in biological samples such as human serum and urine
25 samples. The GR-CS composite modified electrode shows 6 folds enhanced oxidation peak current
26 response with low potential for the detection of DA than that of electrodes modified with bare, GR
27 and CS discretely. Under optimum conditions, the fabricated GR-CS composite modified electrode
28 shows the DPV response of DA in the linear response ranging from 0.03 to 20.06 μM . The
29 detection limit and sensitivity of the sensor was estimated as 0.0045 μM and 6.06 $\mu\text{A } \mu\text{M}^{-1} \text{ cm}^{-2}$.

30 **Keywords:** Graphite; chitosan; biopolymer; dopamine; electro-oxidation; differential pulse
31 voltammetry.

32 **1. Introduction**

33 Over the past few decades, the development of biosensors and chemical sensors for the detection
34 of neurotransmitters has received a great interest due to the vital role in the metabolic system of
35 mammals (Pradhan et al., 2014; Jackowska and Krysinski, 2013). In particular, dopamine (DA) is
36 a well-known inhibitory neurotransmitter and plays an important role in the central nervous system
37 of the human (Nagatsu and Ichinose, 1999). In general, the DA level in the cerebrospinal fluid
38 (CSF) is in the range between 0.5 to 25 nM (Suominen et al., 2013). Furthermore, the malfunctions
39 of DA in CSF leads to many diseases such as Parkinsonism, schizophrenia, hypertension and
40 pheochromocytoma (Ge et al., 2009). Therefore, the levels of DA in blood or urine are essential
41 indicators in medical diagnostics for the diseases. To date, different analytical techniques have
42 been utilized for the reliable determination of DA in biological fluids, such as liquid
43 chromatography (Meng et al., 2000), capillary electrophoresis (Wey and Thormann, 2001), liquid
44 chromatography coupled with UV detection (Ary and Rona, 2001), calorimetry (Secor and Glass,
45 2004), native fluorescence detection (Zhang et al., 2000) and electrochemical methods (Raj et al.,
46 2003; Cabrita et al., 2005). However, the electrochemical methods are simple, rapid, cost-effective
47 and efficient method for determination of DA than that of available traditional methods
48 (Pandikumar et al., 2014).

49 In electrochemical DA sensors, the unmodified electrodes such as glassy carbon, graphite
50 (GR) and screen printed carbon electrodes are not suitable for detection of DA, due to their poor
51 selectivity, reproducibility, sensitivity and high overpotentials (Ghanbari and Hajheidari, 2015;
52 Chen and Cha, 1999). Therefore, the carbon materials, metal oxide, metal alloy nanoparticles,
53 redox and biopolymers modified electrodes have been widely used for the sensitive and selective
54 detection of DA in lower overpotential (Pandikumar et al., 2014; Mao et al., 2015; Yan et al., 2015;

55 Li et al., 2015; Vasantha and Chen, 2006; Wang et al., 2006). On the other hand, chitosan (CS) is
56 known non-toxic, highly biodegradable, naturally abundant linear carbohydrate biopolymer and
57 widely used in the construction of electrochemical sensors and biosensors. Its various potential
58 applications include, tissue engineering, artificial skin, burn treatment, wound healing, drug
59 delivery, (Mertins and Dimova, 2013, 29; Rinaudo, 2006; Vusa et al., 2016). Recently, the CS
60 functionalized graphene oxide and CS grafted graphene and carbon nanotubes have been used for
61 the sensing of DA among its various applications (Shan et al., 2010; Demirkol and Timur, 2011;
62 Liu et al., 2012; Wu et al., 2007; Niu et al., 2012). However, most of the reported DA sensors are
63 based on CS with pristine graphene and or with carbon nanotubes, in which the composites are
64 prepared by the direct sonication of graphene or carbon nanotubes in CS solution (Liu et al., 2012;
65 Niu et al., 2012; Liu et al., 2014). More recently, we have reported DA sensor using the
66 cyclodextrin grafted GR composite, and the resulting electrode has showed comparable
67 performance over carbon nanomaterials modified electrodes for sensing of DA (Palanisamy et al.,
68 2016). The motivation of the present work is to fabricate a simple, sensitive and reliable DA sensor
69 using the CS grafted GR (GR-CS) composite modified electrode. The CS-GR composite can be
70 easily prepared by sonication of GR and CS in acetic acid for 1 h at room temperature. Fewer
71 reports have already reported for the preparation of CS grafted expanded GR (Jagiello et al., 2014;
72 Demitri et al., 2015). However, for the first time we report a potential application of the GR-CS
73 composite for the electrochemical sensing of DA.

74 In this work, a sensitive and selective DA sensor was developed based on GR-CS
75 composite modified electrode for the first time. The GR-CS composite modified electrode shows
76 an enhanced sensitivity with lower oxidation peak potential for DA than that of pristine GR and
77 CS modified electrodes. In addition, the GR-CS modified electrode shows a superior performance

78 towards the oxidation of DA than graphene-CS composite, due to its strong intercalation of CS on
79 exfoliated GR sheets. The selectivity and stability of the sensor were studied and discussed in
80 detail. The practicability of the sensor also been evaluated in biological samples and discussed.

81 **2. Experimental**

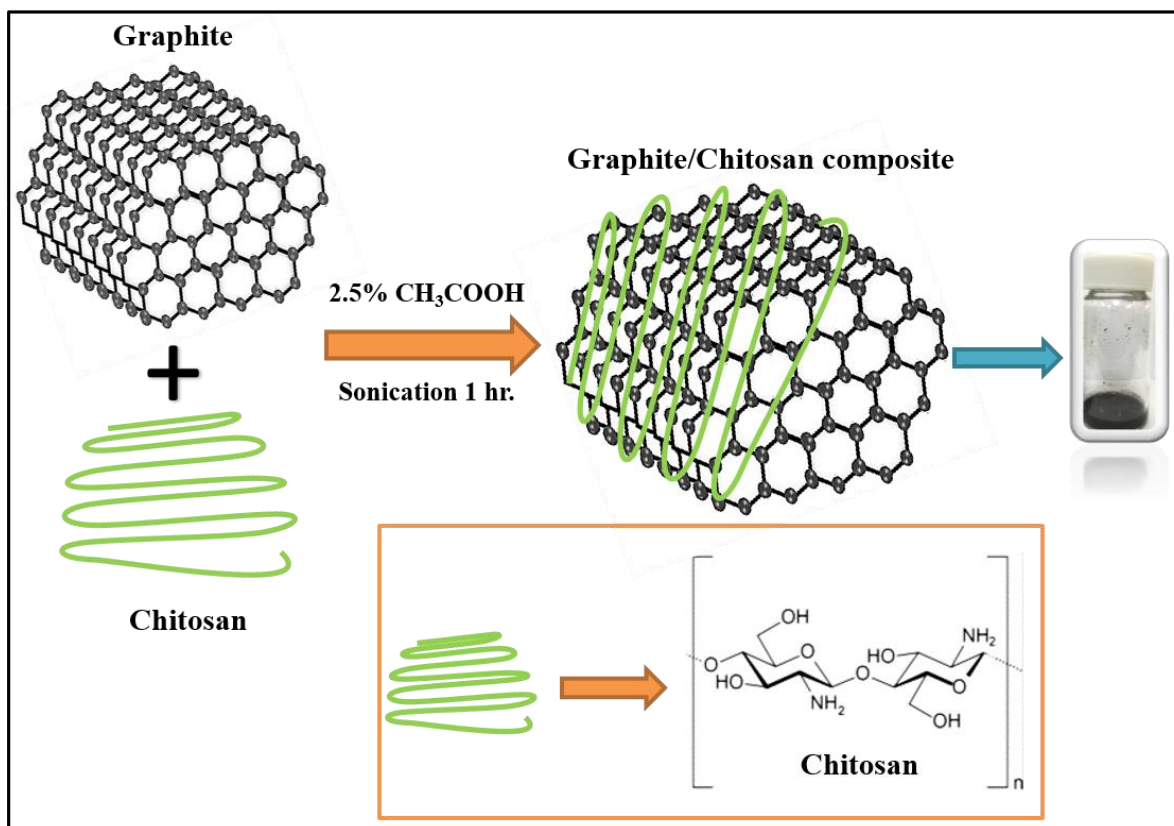
82 *2.1. Chemicals*

83 Raw graphite, dopamine and chitosan (from crab shells, minimum 85% deacetylated) were
84 obtained from Sigma. Uric acid, ascorbic acid and acetic acid were purchased from Aldrich.
85 Graphene nanopowder (8 nm flakes, product number UR-GNAPHENE) was purchased from
86 UniRegion Bio-Tech, Taiwan. Human blood serum sample was collected from valley biomedical,
87 Taiwan product & services, Inc. This study was reviewed and approved by the ethics committee
88 of Chang-Gung memorial hospital through the contract no. IRB101-5042A3 (Palanisamy et al.,
89 2016). Human urine sample were collected from the two healthy persons and used for real sample
90 analysis with their permission. The supporting electrolyte 0.05 M phosphate buffer pH 7 (PBS)
91 was prepared by using 0.05 M Na_2HPO_4 and NaH_2PO_4 solutions in doubly distilled water and the
92 pH were adjusted using 0.1 M H_2SO_4 and NaOH. All chemicals used in this study were of
93 analytical grade and the solutions were prepared using double distilled water without any further
94 purification.

95 *2.2. Apparatus*

96 Cyclic voltammetry (CV) and differential pulse voltammetry (DPV) measurements were
97 performed by the CHI 750a electrochemical work station. Scanning electron microscopy (SEM)
98 was performed using Hitachi S-3000 H electron microscope. Raman spectra were recorded using
99 a Raman spectrometer (Dong Woo 500i, Korea) equipped with a charge-coupled detector. Fourier
100 transform infrared spectroscopy (FT-IR) was carried out using the Thermo SCIENTIFIC Nicolet

101 iS10 instrument. Conventional three-electrode system was used for the electrochemical
102 experiments, the glassy carbon electrode (GCE) with geometric surface area of 0.079 cm² was
103 used as a working electrode, a saturated Ag/AgCl as a reference electrode and a platinum electrode
104 as the auxiliary electrode. All electrochemical measurements were carried out at room temperature
105 in N₂ atmosphere.



106
107 **Scheme 1** Schematic representation of preparation of GR-CS composite.

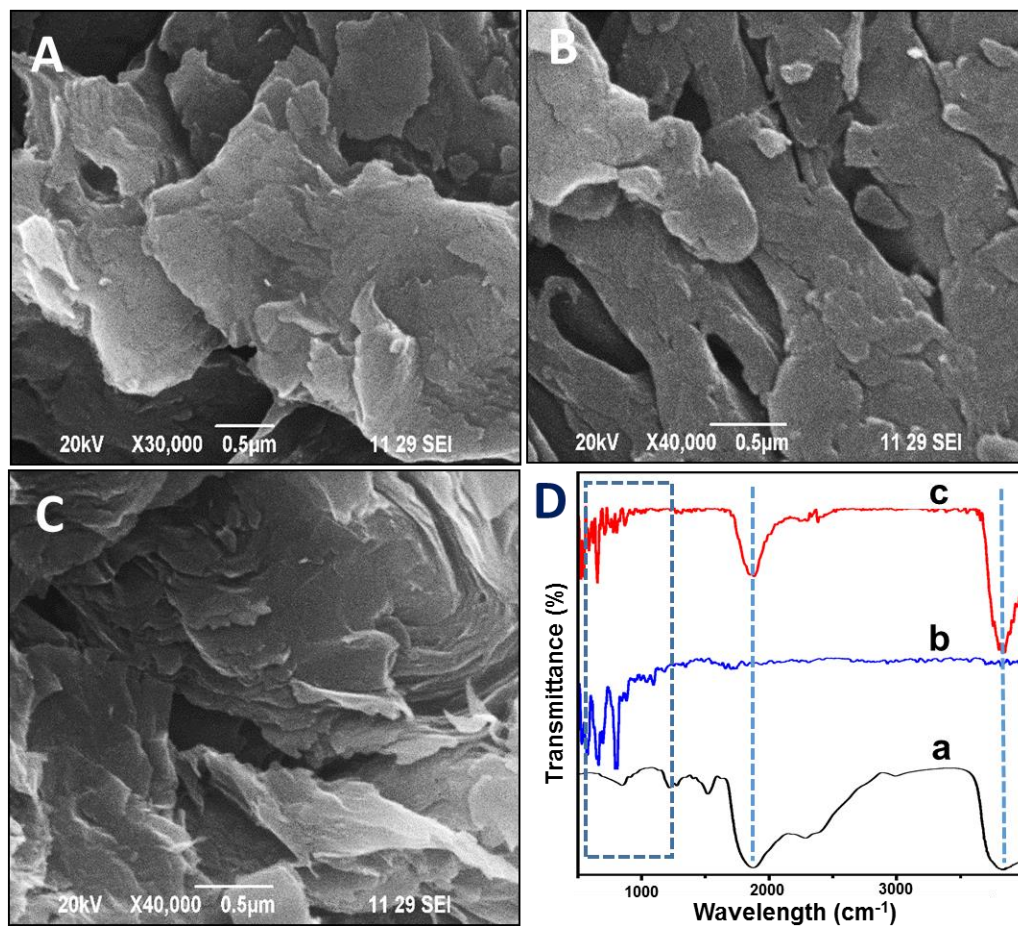
108 *2.3. Preparation of GR-CS composite*

109 To prepare the CS-GR composite, first 15 mg of CS was dissolved in 3 mL of 2.5% acetic acid
110 with the aid of ultra-sonication. Then, 10 mg GR (2:3 w/w, optimum) was added to the CS solution
111 and continuously sonicated for 1 h at room temperature. The resulting GR-CS composite was
112 centrifuged and dried in an air oven. The GR-CS composite was re-dispersed in ethanol and used
113 for further electrochemical experiments. The preparation of CS-GR composite is shown in **Scheme**

114 1. For controls, GR solution was prepared by dispersing 10 mg of GR in dimethylformamide and
115 CS solution was prepared by dissolving 15 mg of CS in 2.5% acetic acid. To prepare GR-CS
116 modified electrode, about 9 μL (optimum) of GR-CS dispersion was drop coated onto pre-cleaned
117 GCE and dried in room temperature. The GR and CS modified GCEs were independently prepared
118 by drop coating of 9 μL of GR and CS on pre-cleaned GCE. For comparison with graphene-CS
119 modified GCE, about 9 μL of the graphene-CS dispersion was drop casted on bare GCE and dried
120 in an air oven. The graphene-CS dispersion was prepared by dispersing of 10 mg of graphene into
121 the CS solution (2:3 w/w) with the help of ultrasonication for 1 h at room temperature.

122 3. Results and discussion

123 3.1. Characterization of GR-CS composite

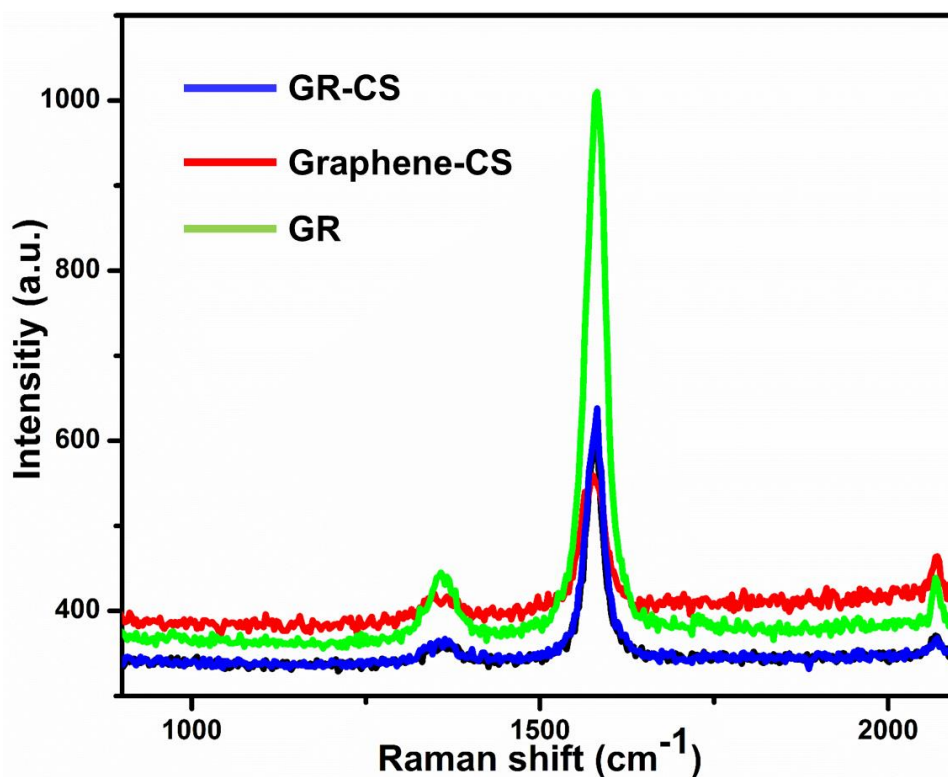


124

125 **Fig. 1** SEM images of (A) pristine GR, B) CS and CS-GR (C). D) FT-IR spectra of CS (a), GR (b)
126 and GR-CS (c).

127 The surface morphology of GR, CS and GR-CS composite was characterized by SEM. **Fig.**
128 **1** displays the SEM images of GR (A), CS (B) and GR-CS composite (C). The SEM image of GR
129 reveals its typical flake sheet morphology with an association of micro graphitic sheets. On the
130 other hand, the SEM image of CS reveals the uniform, thin and porous nature of CS. The SEM of
131 GR-CS composite shows that the GR sheets were well separated and grafted with the highly porous
132 thin film of CS. According to earlier studies, the CS macromolecule is enable to separate graphite
133 layers and prevent the agglomeration of graphite (Jagiello et al., 2014). Typically, the electron pair
134 on nitrogen in CS is in protonated form that enable the CS to strongly interact with graphite sheets,
135 since graphite is known for electron donors (Jagiello et al., 2014). The similar phenomenon has
136 been reported earlier for CS with graphene and GR. The formation of GR-CS composite was
137 further confirmed by FTIR. **Fig. 1D** displays the FTIR spectra of CS (a), GR (b) and GR-CS (c).
138 The FT-IR spectrum of CS depicts characteristic absorption band at 3811 and 3072 cm^{-1} , is
139 attributed to the stretching vibrations of -OH. The absorption band at 1525, 1292 and 1114 cm^{-1} ,
140 attributed to stretching vibrations of C-O-N and C-O, respectively (Liu et al., 2006). In addition,
141 two additional bands are observed at 1184 and 841 cm^{-1} , which is due to the glycosidic bonding
142 of CS (Jagiello et al., 2014). On the other hand, the FTIR spectrum of GR show the bands at 1369
143 and 887 cm^{-1} , which is due to the -CH- bending vibration of GR. The absorption band of CS at
144 1525 cm^{-1} for C-O-N was disappeared when mixed with GR, and the absorption band at 1369 cm^{-1}
145 for C-H stretch was shifted towards 1362 cm^{-1} . This is possibly due to the strong chemical
146 interactions between the CS and GR and result into the exfoliation of GR sheets (Gedam et al.,

147 2015). In addition, the observed other absorption bands of GR-CS composite are consistent with
148 the absorption bands of CS and GR, which confirms that the presence of CS in GR-CS composite.



149
150 **Fig. 2 A)** Raman spectra of GR-CS (blue line), pristine GR (green line) and graphene-CS (red line).

151 Raman spectroscopy was further employed for characterization of GR and GR-CS
152 composite and the results were compared with the Raman spectra of graphene-CS composite. **Fig.**
153 **2** shows the Raman spectra of GR (green profile), GR-CS (blue profile) and graphene-CS (red
154 line). The G band is corresponding to the first-order scattering of the E_{2g} mode in-phase vibration
155 of the graphite lattice and D band is due to the out-of-plane breathing mode of the sp² atoms of
156 graphite (Jagiello et al., 2014). The Raman spectrum of pure GR shows the weak D and strong G
157 bands at 1354 and 1579 cm⁻¹. The D and G bands of CS grafted GR appears at 1363 and 1583 cm⁻¹
158 ¹, and the G band was greatly reduced after the introduction of CS on GR. In addition, the Raman

159 spectra of GR-CS composite is quite similar to the Raman spectra of graphene-CS composite. The
160 result indicates that the successful transformation of GR by CS in GR-CS composite.

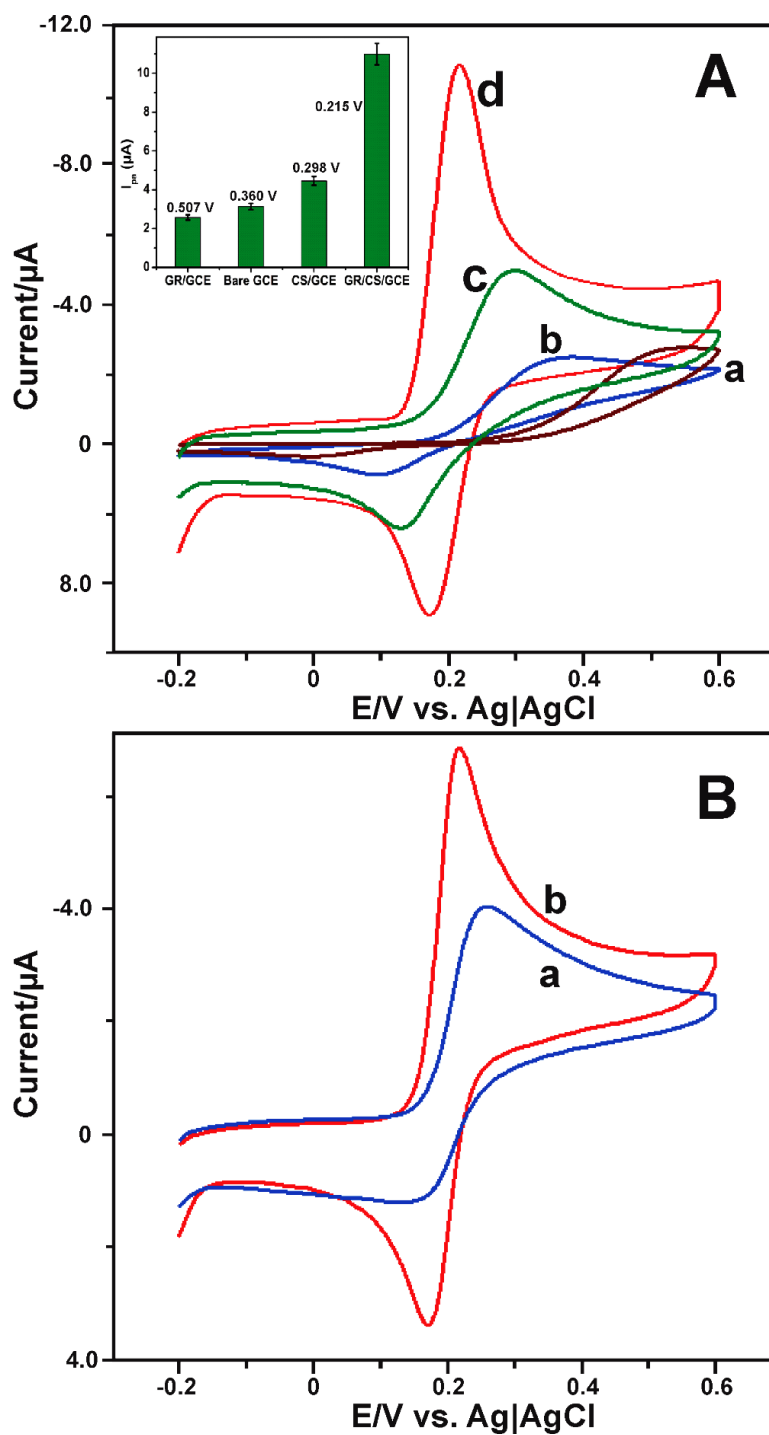
161 3.2. Electrochemical behavior of DA

162 CV was used to investigate the electrochemical behaviour of DA at GR-CS composite modified
163 electrode. **Fig. 3A** shows the CV response of GR (a), bare (b), CS (c) and GR-CS (d) modified
164 electrodes in 50 μM of DA containing PBS at a scan rate of 50 mV s^{-1} . The bare and GR modified
165 electrodes exhibited a weak redox couple for DA and the oxidation peak potential (E_{pa}) of DA was
166 observed at 0.507 and 0.360 V. The E_{pa} of DA was greatly deduced upon the introduction of CS
167 on GCE, the E_{pa} of DA was observed at 0.298 V. In addition, the redox behaviour of DA is greatly
168 enhanced when compared to the response observed in bare and GR modified electrodes. The result
169 indicates the efficient electron transfer ability of CS towards the electrode surface. However, GR-
170 CS composite modified electrode shows a pair of well-defined quasi-reversible redox peak for DA
171 and the E_{pa} of DA was observed at 0.215 V. The observed E_{pa} of DA was 0.292, 0.145 and 0.083
172 V lower than that of GR, bare and CS modified electrodes. Furthermore, the oxidation peak current
173 (I_{pa}) response of DA at GR-CS composite electrode was 4.2, 3.7 and 2.7 folds higher than the
174 response observed in GR, bare and CS modified electrodes (**Fig. 3A inset**). The result indicates
175 that GR-CS composite modified electrode has high electrocatalytic activity towards DA than that
176 of other modified electrodes.

177 As reported earlier that the protonated form of CS in acidic acid solution could easily
178 interact with the p electrons in sp^2 hybrid orbital of GR (Jagiello et al., 2014). In addition, the long
179 chain of CS is more favourable to interact with each graphitic sheets in GR and result into
180 exfoliation of GR. The exfoliated GR in GR-CS composite contains high number of basal planes
181 per volume, while the amount of available edge plane remains the same (Figueiredo-Filho et al.,

182 2013). The large number of basal planes in GR-CS composite and result into the high surface area
183 and high electrocatalytic activity towards DA. Furthermore, the distinct structure of CS plays an
184 important role to prevent the accumulation of exfoliated GR in GR-CS composite (Jagiello et al.,
185 2014). In order to further clarify the catalytic activity, the electrocatalytic behaviour of DA at
186 GR/CS composite was compared with graphene-CS composite. **Fig. 3B** shows CV responses of
187 graphene/CS (a) and GR-CS (b) modified electrodes in PBS containing 25 μM of DA in PBS at a
188 scan rate of 50 mV s^{-1} . A well-defined quasi redox couple was observed for DA at graphene/CS
189 composite modified electrode and the oxidation peak of DA was appeared at 0.284 V. However,
190 the GR-CS modified electrode shows 2 folds enhanced oxidation peak current and lower
191 overpotential (0.215 V) for detection of DA than that of graphene/CS composite modified
192 electrode. It is evident from the result that the GR-CS composite has quite higher or similar
193 electrocatalytic activity to graphene/CS modified electrode.

194 The CS grafted GR composite mostly exists in positive form when the pH was below 5 due
195 to the protonation of $-\text{NH}_2$ group of CS (Jiang et al., 2004). While, the protonation of $-\text{NH}_2$ group
196 is very low when the pH was more than 6.0, this is more favourable for H-bond interactions
197 between CS and DA (Jiang et al., 2004). These are the possible reasons for enhanced
198 electrochemical behavior and lower oxidation potential of DA at GR-CS composite. We have also
199 investigated the electrochemical behaviour DA at graphene/CS composite and the results are
200 compared with the response observed at GR-CS composite.



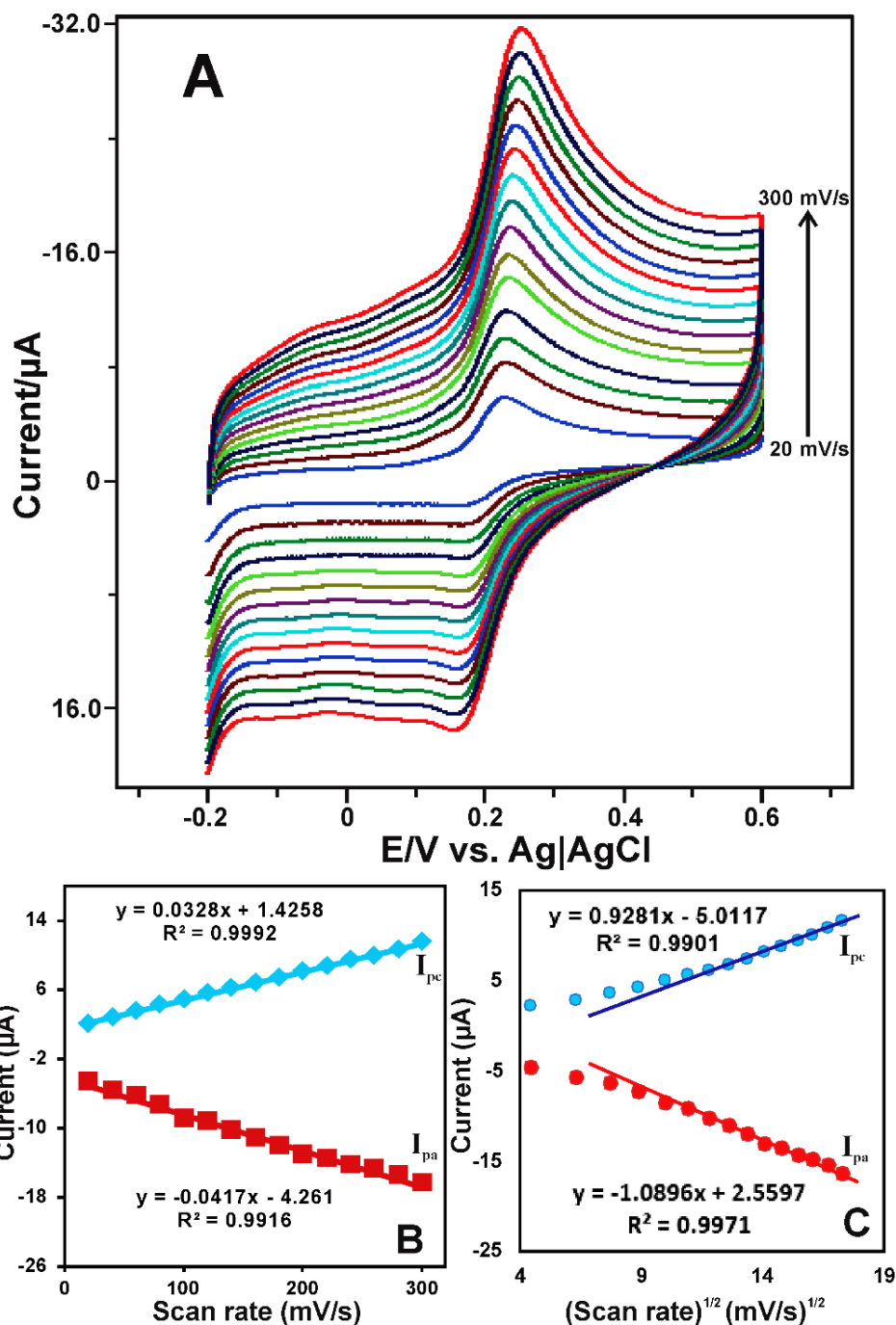
201
 202 **Fig. 3** A) CV response of the GR (a), bare (b), CS (c) and GR-CS (d) modified GCEs in 50 μM of
 203 DA containing PBS at a scan rate of 50 mV s⁻¹. Inset shows the I_{pa} and E_{pa} of DA vs. different
 204 modified electrodes. B) At the same conditions, CV response of the graphene-CS (a) and GR-CS
 205 (b) modified GCEs in 25 μM of DA containing PBS at a scan rate of 50 mV s⁻¹.

206 *3.3. Optimization*

207 The optimization studies are more important and it may directly affect the electrochemical
208 behaviour of DA. Hence, the optimization of GR, CS in GR-CS composite and drop coating
209 amount of GR-CS composite towards the detection of 50 μM DA was investigated by CV. The
210 experimental conditions are similar as of in **Fig. 3A**. The optimization results are shown in **Fig.**
211 **S1A-C**. It can be seen from **Fig. S1A** and **B** that the high sensitivity of DA was observed for 2 and
212 3 wt% of GR and CS containing GR-CS composite. We have used GR and CS loading as 2 and 3
213 wt% for optimize the GR and CS. Hence, the 2 and 3 wt% of GR and CS was used for the
214 preparation of GR-CS composite. In the same manner, 9 μL drop coated GR-CS composite
215 modified electrode showed a maximum current response for DA than that of other drop coated
216 electrodes (**Fig. S1C**). Hence, 9 μL drop coated GR-CS composite modified electrode was used as
217 an optimum quantity for further electrochemical investigations.

218 *3.4. Effect of scan rate and pH*

219 The effect of scan rate on the electrochemical behaviour of 50 μM DA was investigated in PBS by
220 CV. **Fig. 4A** shows the CV response of GR-CS modified electrode in 50 μM DA containing PBS
221 at different scan rates from 10 to 300 mV s^{-1} . It can be seen that the I_{pa} and cathodic peak current
222 (I_{pc}) of DA increases with increasing the scan rate from 10 to 300 mV s^{-1} .



223
 224 **Fig. 4** A) CV response obtained at GR-CS modified electrode in the presence of 50 μM DA
 225 containing PBS at different scan rates from 10 to 300 mV/s. B) Linear dependence of scan rate vs.
 226 I_{pa} . C) Linear plot of square root of scan rate vs. I_{pa} .

227 Furthermore, I_{pa} and I_{pc} had exhibited a linear relationship with a scan rate from 10 to 300
 228 mV s^{-1} (**Fig. 4B**), which indicates that the electrochemical behaviour of DA is controlled by a

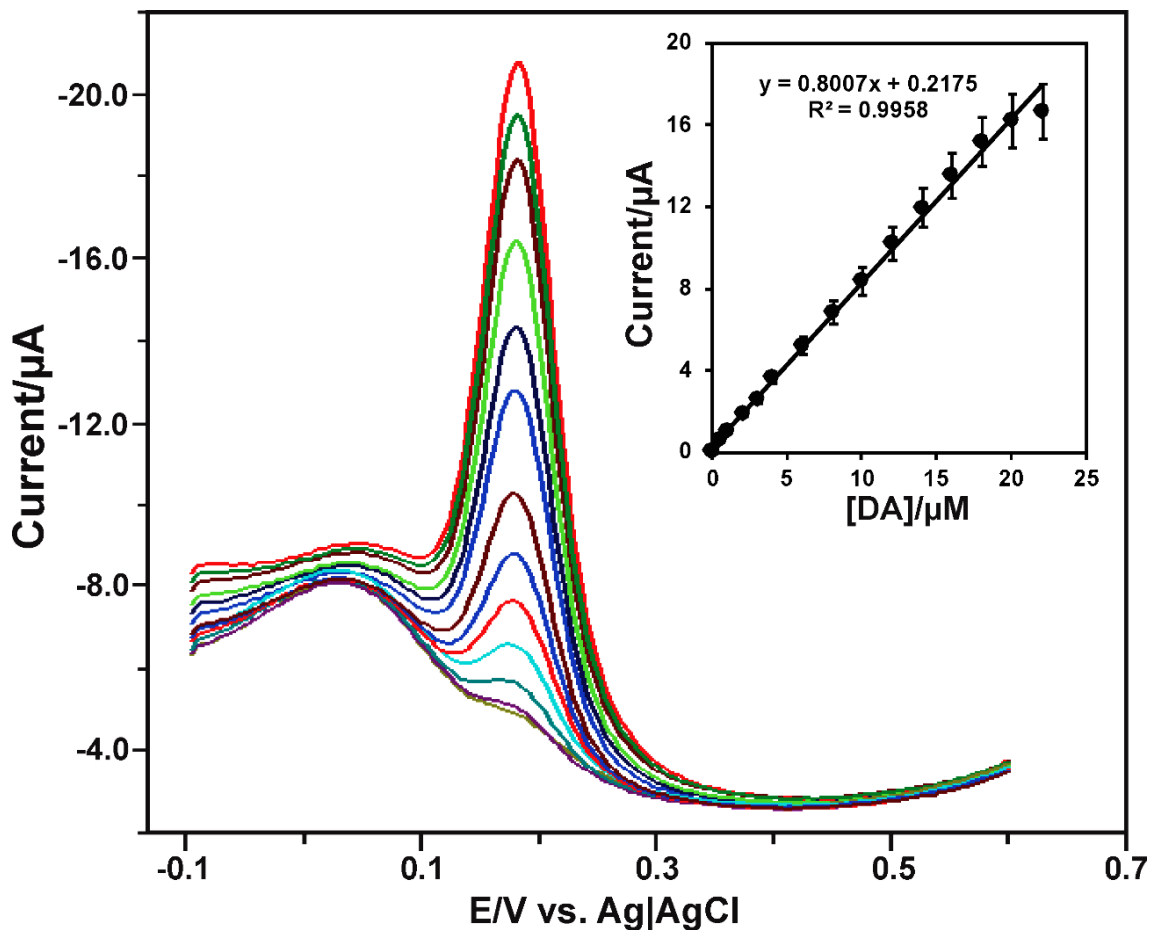
229 typical adsorption-controlled process. However, the (I_{pa}) and (I_{pc}) are linearly proportional to the
230 square root of the scan rates from the scan rates from 120 to 300 mV s^{-1} (**Fig. 4C**), indicating that
231 electrochemical behaviour of DA is a diffusion controlled process at higher scan rates. The above
232 result confirms that the electrochemical behaviour of DA at GR-CS composite modified electrode
233 is controlled by a mixed kinetic process.

234 The electrochemical redox behaviour of 75 μM DA was investigated using the GR-CS
235 composite modified electrode in different pH solutions by CV. **Fig. S2A** shows the CV response
236 of GR-CS composite modified electrode in different pH solutions (pH 3, 5, 7, 9 and 11) containing
237 75 μM of DA at a scan rate of 50 mV s^{-1} . A well-defined redox couple of DA was observed in
238 each pH and the E_{pa} and reduction peak potential (E_{pc}) were shifted towards negative and positive
239 direction upon increasing and decreasing the pH. Furthermore, the E_{pa} and E_{pc} of DA had a linear
240 relationship between the pH from 3 to 11, as shown in **Fig. S2B**. The linear plot was derived
241 against the formal potential ($E^{0'} = (E_{pa} + E_{pc})/2$) vs. pH and the slope value was found as 58.6
242 mV/pH with the correlation coefficient of 0.9854. The observed slope value is close to the
243 theoretical slope value for an equal number of protons and electrons transferred electrochemical
244 reaction, as reported previously (Palanisamy et al., 2016). The electrochemical mechanism of DA
245 at carbon modified electrodes have been well demonstrated and the redox behaviour of DA at GR-
246 CS composite involves two protons and two electrons coupled electrochemical reaction.

247 *3.5. Determination of DA and selectivity of the biosensor*

248 DPV was employed for the electrochemical determination of DA using the GR-CS composite
249 modified electrode. **Fig. 5** shows the typical DPV response of the GR-CS composite modified
250 electrode for the absence and presence of additions of different concentration of DA into the PBS.
251 It can be seen that the GR-CS composite modified electrode did not show any apparent response

252 in the absence of DA. However, a sharp oxidation peak response was observed for the addition of
253 DA from 0.05 to 22.06 μM . As shown in **Fig. 5 inset**, the GR-CS composite exhibited the response
254 current of DA was linear over the concentration ranging from 0.03 to 20.06 μM with the correlation
255 coefficient of 0.9958.



256
257 **Fig. 5 A)** DPV response of the GR-CS electrode for the additions of different concentration of DA
258 into the PBS. Inset: Linear relationship of I_{pa} vs. [DA]. DPV conditions are: sampling width:
259 0.0167 s; pulse width: 0.05 s; pulse period: 0.2 s; amplitude: 0.05 V; quiet time: 2 s.

260 The sensitivity of the developed sensor was estimated to be $6.06 \mu\text{A}\mu\text{M}^{-1} \text{cm}^{-2}$ based on the
261 slope value of the calibration plot. The GR-CS composite modified electrode active surface area
262 was 0.12 cm^2 . The limit of detection (LOD) was estimated as $0.0045 \mu\text{M}$ based on $S/N=3$. The

263 fabricated DA sensor exhibited low LOD for DA when compared to sulphonated CS (Vusa et al.,
264 2016), CS entrapped graphene (Niu et al., 2012; Liu et al., 2014; 36. Weng et al., 2013; Han et al.,
265 2010; Liu et al., 2011; Wang et al., 2013) and carbon nanotubes modified electrodes (Babaei et al.,
266 2011), as shown in **Table ST1**. On the other hand, the obtained linear range of our sensor was quite
267 narrow when compared to the previously reported modified electrodes for the detection of DA. We
268 have also compared the analytical performance of the present DA sensor with previously reported
269 tyrosinase based different DA sensors and the comparative results are shown in Table. S2. The
270 comparison results clear that the fabricated DA sensor shows high sensitivity and comparable LOD
271 and linear response for the detection of DA (Maciejewska et al., 2011; Zhou et al., 2007; Tsai et al.,
272 2007; Tembe et al., 2008; Njagi et al., 2008; Min and Yoo, 2009; Njagi et al., Forzani et al., 1995;
273 Hasebe et al., 1995; Cosnier et al., 1997; Pandey et al., 2001; Ve´drine et al., 2003; Tembe et al.,
274 2006; Wang, et al., 2010). In addition, the developed DA sensor is less expensive and easy to
275 prepare when compared with previously enzymatic and non-enzymatic DA sensors (Jackowska and
276 Krysinski, 2013).

277 The selectivity of the modified electrode is much important for the detection of DA in the
278 presence of potentially active compounds which are commonly present in biological samples, such
279 as ascorbic acid (AA) and uric acid (UA). These compounds can potentially interfere the response
280 of DA on the modified electrode due to their close oxidation potential with DA. Hence, the
281 selectivity of GR-CS composite modified electrode towards the detection of DA was evaluated in
282 the presence of AA and UA by DPV. The selectivity results are shown in **Fig. S3**. The experimental
283 conditions and DPV working parameters are similar as of in **Fig. 5**. The GR-CS composite
284 modified electrode shows a sharp oxidation peak at 0.194 V for the addition of 1 μ M DA (a). while,
285 100 μ M addition of AA (b) do not show any electrochemical response on the same potential

286 window. In addition, the response current and peak potential of DA was not affected in the
287 presence of 100 μM AA, which clearly indicates that AA do not have cross reactivity with DA.
288 On the other hand, the GR-CS composite modified electrode shows a tiny response at 0.384 V for
289 the presence of 30 μM UA, and the response current of UA increases with the addition of 50, 100
290 and 200 μM of UA into the PBS. The oxidation peak current response of DA slightly affected in
291 the presence of UA, while the peak potential of DA unaffected even in the presence of 200 μM
292 UA. The protonation of $-\text{NH}_2$ group of CS in GR-CS composite is very weak when the pH was
293 more than 6.0, hence the H-bonding is more favourable towards DA than that of interaction with
294 UA and AA. This is the possible reasons for high selectivity of the GR-CS composite towards the
295 detection of DA. The result clearly demonstrates the high selectivity of the fabricated DA sensor.

296 *3.6. Determination of DA in biological samples*

297 The practical ability of GR-CS composite modified electrode was evaluated by determination of
298 DA in biological samples such as human blood serum and urine samples. The standard addition
299 method was used for the determination of DA in human blood serum and urine samples. The DPV
300 was used for the determination of DA and the experimental conditions are similar as of in **Fig. 5**.
301 The human urine samples were diluted 10 times before the DPV measurements. The unknown
302 concentration of DA was predetermined in DA containing spiked human serum and urine samples
303 by DPV. Then, the known concentration of DA (2 μM) containing human blood serum and urine
304 samples was spiked into the PBS. The obtained recovery results are summarized in **Table ST3**.
305 The GR-CS composite modified electrode showed the average recovery of DA about 98.3 and
306 100.5 % DA in the human blood serum and urine samples. The result confirmed that the GR-CS
307 composite modified electrode could be used for the reliable detection of DA in biological real
308 samples.

309 The stability of the GR-CS composite modified electrode was examined periodically
310 towards the detection of 50 μM of DA by CV for 6 days. The GR-CS composite modified electrode
311 retains 93.6% of the initial current response of DA (figure not shown) after the storage (6 days) in
312 PBS at 4 °C. The result indicates the good stability of the GR-CS composite modified electrode
313 towards the detection of DA. The reproducibility and repeatability of the GR-CS composite
314 modified electrode towards the detection of DA was evaluated by CV. The relative standard
315 deviation (RSD) of 2.9% was found for 10 measurements of 50 μM DA by single GR-CS
316 composite modified electrode. The five independently prepared GR-CS composite modified
317 electrode shows the RSD of 4.3% for the detection of 50 μM DA. The results indicate that GR-CS
318 composite modified electrode has good repeatability and reproducibility for the detection of DA.

319 **4. Conclusions**

320 We have reported a simple and reliable DA sensor using the GR-CS composite modified
321 electrode for the first time. The modified electrode showed high catalytic activity and lower
322 oxidation potential towards the detection of DA, which is attributed to the excellent conductivity
323 and adsorption property of GR and CS. The as-prepared GR-CS composite modified electrode
324 shows a high sensitivity, low LOD, appropriate response range and satisfactory stability for the
325 detection of DA. The GR-CS composite modified electrode has many practical advantages over
326 the reported nanomaterials modified electrodes for the detection of DA, such as cost-effective,
327 highly reproducible and can be prepared in short period of time (1 h). The fabricated electrode
328 showed high selectivity towards DA in the presence of excess addition of AA and UA. The good
329 recovery of DA in human serum and in urine samples authenticates that the fabricated GR-CS
330 composite electrode is well suitable for the detection DA for biological and medicinal applications.

331 **Acknowledgments**

332 This project was supported by the Ministry of Science and Technology, Taiwan (Republic of
333 China).

334

335 **References**

- 336 Ary, K., & Rona, K. 2001. LC determination of morphine and morphine glucuronides in human
337 plasma by coulometric and UV detection, *J. Pharm. Biomed. Anal.*, 26, 179–187.
- 338 Babaei, A., Babazadeh, M., & Momeni, H.M. 2011. A sensor for simultaneous determination of
339 dopamine and morphine in biological samples using a multi-walled carbon
340 nanotube/chitosan composite modified glassy carbon electrode, *Int. J. Electrochem. Sci.*,
341 6,1382–1395.
- 342 Cabrita, J.F., Abrantes, L.M., & Viana, A.S. 2005. N-Hydroxysuccinimide-terminated self-
343 assembled monolayers on gold for biomolecules immobilization, *Electrochim. Acta.*, 50,
344 2117–2124.
- 345 Chen, J., & Cha, C.S. 1999. Detection of dopamine in the presence of a large excess of
346 ascorbic acid by using the powder microelectrode technique, *J. Electroanal. Chem.*,
347 463, 93–99.
- 348 Cosnier, S., Innocent, C., Allien, L., Poitry, S., & Tsacopoulos, M. 1997. An electrochemical
349 method for making enzyme microsensors. application to the detection of dopamine and
350 glutamate, *Anal. Chem.*, 69, 968–971.
- 351 Demirkol, D.O., & Timur, S. 2011. Chitosan matrices modified with carbon nanotubes for use
352 in mediated microbial biosensing, *Microchim. Acta.*,173, 537–542.
- 353 Demitri, C., Moscatello, A., Giuri, A., Raucci, M.G., & Corcione, C.E. 2015. Preparation and
354 characterization of eg-chitosan nanocomposites via direct exfoliation: a green
355 methodology, *Polymers.*, 7, 2584–2594.

356 Figueiredo-Filho, L.C.S., Brownson, D.A.C., Mingot, M.G., Iniesta, J., Fatibello-Filho, O., &
357 Banks, C.E. 2013. Exploring the electrochemical performance of graphitic paste electrodes:
358 graphene vs. graphite, *Analyst.*, 138, 6354–6364.

359 Forzani, E.S., Rivas, G.A., & Solis, V.M. 1995. Amperometric determination of dopamine on
360 an enzymatically modified carbon paste electrode, *J. Electroanal. Chem.*, 382, 33–40.

361 Ge, B., Tan, Y., Xie, Q., Ma, M., & Yao, S. 2009. Preparation of chitosan–dopamine-multiwalled
362 carbon nanotubes nanocomposite for electrocatalytic oxidation and sensitive
363 electroanalysis of NADH, *Sens. Actuators B.*, 137, 547–554.

364 Gedam, A.H., Dongre, R.S., & Bansiwala, A.K. 2015. Synthesis and characterization of graphite
365 doped chitosan composite for batch adsorption of lead (II) ions from aqueous solution, *Adv.
366 Mater. Lett.*, 6, 59–67.

367 Ghanbari, K., & Hajheidari, N. 2015. ZnO–Cu₂O/polypyrrole nanocomposite modified
368 electrode for simultaneous determination of ascorbic acid, dopamine, and uric acid, *Anal.
369 Biochem.*, 473, 53–62.

370 Han, D., Han, T., Shan, C.S., Ivaska, & A., Niua, L. 2010. Simultaneous determination of
371 ascorbic acid, dopamine and uric acid with chitosan-graphene modified electrode,
372 *Electroanalysis.*, 22, 2001–2008.

373 Hasebe, Y., Hirano, T., & Uchiyama, S. 1995. Determination of catecholamines and uric acid in
374 biological fluids without pretreatment, using chemically amplified biosensors, *Sens.
375 Actuators, B.*, 24-25, 94–97.

376 Jackowska, K., & Kryszewski, P. 2013. New trends in the electrochemical sensing of dopamine,
377 *Anal. Bioanal. Chem.*, 405, 3753–3771.

378 Jagiello, J., Judek, J., Zdrojek, M.M., Aksienionek, M., & Lipinska, L. 2014. Production of
379 graphene composite by direct graphite exfoliation with chitosan, *Mater. Chem. Phys.*, 148,
380 507–511.

381 Jiang, L., Liu, C., Jiang, L., Peng, Z., & Lu, G. 2004. A chitosan-multiwall carbon nanotube
382 modified electrode for simultaneous detection of dopamine and ascorbic acid, *Anal. sci.*,
383 20, 1055–1059.

384 Li, B., Zhou, Y., Wu, W., Liu, M., Mei, S., Zhou, Y., & Jing, T. 2015. Highly selective and
385 sensitive determination of dopamine by the novel molecularly imprinted poly
386 (nicotinamide)/CuO nanoparticles modified electrode, *Biosens. Bioelectron.*, 67, 121–128.

387 Liu, B., Lian, H.T., Yin, J.F., & Sun, X.Y. 2012. Dopamine molecularly imprinted
388 electrochemical sensor based on graphene–chitosan composite, *Electrochim. Acta.*, 75,
389 108–114.

390 Liu, C., Zhang, J., Yifeng, E., Yue, J., Chen, L., & Li, D. 2014. One-pot synthesis of graphene–
391 chitosan nanocomposite modified carbon paste electrode for selective determination of
392 dopamine, *Electron. J. Biotechnol.*, 17, 183–188.

393 Liu, H., Bao, J., Du, Y., Zhou, X., & Kennedy, J.F. 2006. Hydration energy of the 1, 4-bonds of
394 chitosan and their breakdown by ultrasonic treatment, *Carbohydr. Polym.*, 64, 553–559.

395 Liu, X., Peng, Y., Qua, X., Ai, S., Han, R., & Zhu, X. 2011. Multi-walled carbon nanotube
396 chitosan/poly(amidoamine)/DNA nanocomposite modified gold electrode for
397 determination of dopamine and uric acid under coexistence of ascorbic acid, *J. Electroanal.*
398 *Chem.*, 654, 72–78.

399 Maciejewska, J., Pisareka, K., Bartosiewicz, I., Krysiniski, P., Jackowska, K., & Bieganski, A.
400 T. 2011. Selective detection of dopamine on poly (indole-5-carboxylic acid)/tyrosinase
401 Electrode, *Electrochim. Acta.*, 56, 3700-3706.

402 Mao, H., Liang, J., Zhang, H., Pei, Q., Liu, D., Wu, S., Zhang, Y., & Song, X.M. 2015. Poly
403 (ionic liquids) functionalized polypyrrole/graphene oxide nanosheets for electrochemical
404 sensor to detect dopamine in the presence of ascorbic acid, *Biosens. Bioelectron.*, 70, 289–
405 298.

406 Meng, Q. C., Cepeda, M.C., Kramer, T., Zou, H., Matoka, D.J., & Farrar, J. 2000. High-
407 performance liquid chromatographic determination of morphine and its 3-and 6-
408 glucuronide metabolites by two-step solid-phase extraction, *J. Chromatogr. B.*, 742, 115–
409 123.

410 Mertins, O., & Dimova, R. 2013. Insights on the interactions of chitosan with phospholipid
411 vesicles. part i: effect of polymer deprotonation, *Langmuir.*, 29, 14545–14551.

412 Min, K., & Yoo, Y.J. 2009. Amperometric detection of dopamine based on tyrosinase–SWNTs–
413 Ppy composite electrode, *Talanta.*, 80, 1007–1011.

414 Nagatsu, T., & Ichinose, H. 1999. Molecular biology of catecholamine-related enzymes in
415 relation to Parkinson's disease, *Cell. Mol. Neurobiol.*, 19, 57–66.

416 Niu, X., Yang, W., Guo, H., Ren, J., Yang, F., & Gao, J. 2012. A novel and simple strategy for
417 simultaneous determination of dopamine, uric acid and ascorbic acid based on the stacked
418 graphene platelet nanofibers/ionic liquids/chitosan modified electrode, *Talanta*, 99, 984–
419 988.

420 Njagi, J., Chernov, M.M., Leiter, J.C., & Andreescu, S. 2010. Amperometric detection of
421 dopamine in vivo with an enzyme based carbon fiber microbiosensor, *Anal. Chem.*, 82,
422 989–996.

423 Njagi, J., Ispas, C., & Andreescu, S. 2008. Mixed ceria-based metal oxides biosensor for
424 operation in oxygen restrictive environments, *Anal. Chem.*, 80, 7266–7274.

425 Palanisamy, S., Sakthinathan, S., Chen, S.M., Thirumalraj, B., Wu, T.H., Lou, B.S., & Liu, X.
426 2016. Preparation of β -cyclodextrin entrapped graphite composite for sensitive detection
427 of dopamine, *Carbohydr.Polym.*, 135, 267–273.

428 Pandey, P.C., Upadhyay, S., Tiwari, I., Singh, G & Tripathi, V.S. 2001. A novel ferrocene
429 encapsulated palladium–linked ormosil-based electrocatalytic dopamine sensor, *Sens.*
430 *Actuators, B.*,75, 48–55.

431 Pandikumar, B., How, G.T.S., See, T.P., Omar, F.S., Jayabal, S., Kamali, K.Z., Yusoff, N., Jamil,
432 A., Ramaraj, R., John, S.A., Lim, H.N., & Huang, N.M. 2014. Graphene and its
433 nanocomposite material based electrochemical sensor platform for dopamine, *RSC Adv.*,
434 4, 63296–63323.

435 Pradhan, T., Jung, H.S., Jang, J.H., Kim, T.W., Kang, C., & Kim, J.S. 2014. Chemical sensing
436 of neurotransmitters, *Chem. Soc. Rev.*, 43, 4684–4713.

437 Raj, C. R., Okajima, T., & Ohsaka, T.J. 2003. Gold nanoparticle arrays for the voltammetric
438 sensing of dopamine, *Electroanal. Chem.*, 543, 127–133.

439 Rinaudo, M. 2006. Chitin and chitosan: properties and applications, *Prog. Polym. Sci.*, 31,603–
440 632.

441 Secor, K.E., & Glass, T.E. 2004. Selective amine recognition: development of a chemosensor
442 for dopamine and norepinephrine, *Org. Lett.*, 6, 3727–3730.

443 Shan, C., Yang, H., Han, D., Zhang, Q., Ivaska, A., & Niu, L. 2010. Graphene/AuNPs/chitosan
444 nanocomposites film for glucose biosensing, *Biosens.Bioelectron.*, 25, 1070–1074.

445 Suominen, T., Uutela, P., Ketola, R.A., Bergquist, T., Hillered, L., Finel, M., Zhang, H., Laakso,
446 A., & Kostianen, R. 2013. Determination of serotonin and dopamine metabolites in human
447 brain microdialysis and cerebrospinal fluid samples by UPLC-MS/MS: discovery of intact
448 glucuronide and sulfate conjugates, *PLoS One.*, 8, e68007.

449 Tembe, S., Karve, M., Inamdar, S., Haram, S., Melo, J., & D'Souza, S.F. 2006. Development of
450 electrochemical biosensor based on tyrosinase immobilized in composite biopolymeric
451 film, *Anal. Biochem.*, 349, 72–77.

452 Tembe, S., Kubal, B.S., Karve, M., & D'Souza, S.F. 2008. Glutaraldehyde activated eggshell
453 membrane for immobilization of tyrosinase from *amorphophallus companulatus*:
454 Application in construction of electrochemical biosensor for dopamine, *Anal. Chim. Acta.*,
455 612, 212–217.

456 Tsai, Y.C., & Chiu, C.C. 2007. Amperometric biosensors based on multiwalled carbon nanotube-
457 nafion-tyrosinase nanobiocomposites for the determination of phenolic compounds, *Sens.*
458 *Actuators, B.*, 125, 10–16.

459 Vasantha, V.S., & Chen, S.M. 2006. Electrocatalysis and simultaneous detection of dopamine
460 and ascorbic acid using poly (3, 4-ethylenedioxy) thiophene film modified electrodes, *J.*
461 *Electroanal. Chem.*, 592, 77–87.

462 Ve´drine, C., Fabiano, S., & Minh, C.T. 2003. Amperometric tyrosinase based biosensor using
463 an electrogenerated polythiophene film as an entrapment support, *Talanta.*, 59, 535–544.

464 Vusa, C.S.R., Manju, V., Aneesh, K., Berchmans, S., & Palaniappan, A. 2016. Tailored
465 interfacial architecture of chitosan modified glassy carbon electrodes facilitating selective,
466 nanomolar detection of dopamine, *RSC Adv.*, 6, 4818–4825.

467 Wang, H.S., Li, T.H., Jia, W.L., & Xu, H.Y. 2006. Highly selective and sensitive determination
468 of dopamine using a nafion/carbon nanotubes coated poly(3-methylthiophene) modified
469 electrode, *Biosens. Bioelectron.*, 22, 664–669.

470 Wang, X., Wu, M., Tang, W., Zhu, Y., Wang, L., Wang, Q., He, P., & Fang, Y. 2013.
471 Simultaneous electrochemical determination of ascorbic acid, dopamine and uric acid
472 using a palladium nanoparticle/graphene/chitosan modified electrode, *J. Electroanal.*
473 *Chem.*, 695, 10–16.

474 Wang, Y., Zhang, X., Chen, Y., Xu, H., Tan, Y., & Wang, S. 2010. Detection of dopamine based
475 on tyrosinase-Fe₃O₄ nanoparticles-chitosan nanocomposite biosensor, *Am. J. Biomed. Sci.*,
476 2(3), 209–216.

477 Weng, X., Cao, Q., Liang, L., Chen, J., You, C., Ruan, Y., Lin, H., & Wu, L. 2013. Simultaneous
478 determination of dopamine and uric acid using layer-by-layer graphene and chitosan
479 assembled multilayer films, *Talanta.*, 117, 359–365.

480 Wey, A.B., & Thormann, W. 2001. Capillary electrophoresis–electrospray ionization ion trap
481 mass spectrometry for analysis and confirmation testing of morphine and related
482 compounds in urine, *J. Chromatogr. A.*, 916, 225–238.

483 Wu, Z., Feng, W., Feng, Y., Liu, Q, Xu, X, Sekino, T, Fujii, A., & Ozaki, M. 2007. Preparation
484 and characterization of chitosan-grafted multiwalled carbon nanotubes and their
485 electrochemical properties, *Carbon.*, 45, 1212–1218.

486 Yan, Y., Liu, Q., Du, X., Qian, J., Mao, H., & Wang, K. 2015. Visible light photoelectrochemical
487 sensor for ultrasensitive determination of dopamine based on synergistic effect of graphene
488 quantum dots and TiO₂ nanoparticles, *Anal. Chim. Acta.*, 853, 258–264.

489 Zhang, X.X., Li, J., Gao, J., Sun, L., & Chang, W.B. 2000. Determination of morphine by
490 capillary electrophoresis immunoassay in thermally reversible hydrogel-modified buffer
491 and laser-induced fluorescence detection, *J. Chromatogr. A*, 895, 1–7.

492 Zhou, Y.L., Tian, R.H., & Zhi, J.F. 2007. Amperometric biosensor based on tyrosinase
493 immobilized on a boron-doped diamond electrode, *Biosens. Bioelectron.*, 22, 822–828.

494

495

